Title

Constitutively enhanced genome integrity maintenance and direct stress mitigation characterize transcriptome of extreme stress-adapted *Arabidopsis halleri*

Authors

Gwonjin Lee[a], Julia Quintana, Hassan Ahmadi, Lara Syllwasschy, Nadežda Janina, Veronica Preite, Justin E. Anderson[b], Björn Pietzenuk and Ute Krämer

Affiliations

Molecular Genetics and Physiology of Plants, Ruhr University Bochum, D-44801 Bochum, Germany

Contact Information

Email: Ute.Kraemer@ruhr-uni-bochum.de

Additional Footnotes

Present address: [a]Department of Botany and Plant Pathology, Purdue University, IN, USA; [b]BASF, Napoleonsweg 152, 6083 AB Nunhem, Netherlands

Running title

Intra-species comparative transcriptomics

Abstract

Heavy metal-rich toxic soils and ordinary soils are both natural habitats of *Arabidopsis halleri*. The molecular divergence underlying survival in sharply contrasting environments is unknown. Here we comparatively address metal physiology and transcriptomes of *A. halleri* originating from the most highly heavy metal-contaminated soil in Europe, Ponte Nossa (Noss/IT), and from non-metalliferous (NM) soil. Noss exhibits enhanced hypertolerance and attenuated accumulation of cadmium (Cd), and transcriptomic Cd responsiveness is decreased, compared to plants of NM soil origin. Among the condition-independent transcriptome characteristics of Noss, the most highly overrepresented functional class of "meiotic cell cycle" comprises 21 transcripts with elevated abundance in vegetative tissues, in particular *ARGONAUTE 9* (*AGO9*) and the synaptonemal complex transverse filament protein-encoding *ZYP1a/b*. Increased *AGO9* transcript levels in Noss are accompanied by decreased long terminal repeat retrotransposon expression, and are shared by plants from milder metalliferous sites in Poland and Germany. Expression of *IRON-REGULATED TRANSPORTER1* (*IRT1*) is very low and of *HEAVY METAL ATPASE2* (*HMA2*) strongly elevated in Noss, which can account for its specific Cd handling. In plants adapted to the most extreme abiotic stress, broadly enhanced functions comprise genes with likely roles in somatic genome integrity maintenance, accompanied by few alterations in stress-specific functional networks.

Keywords: heavy metal, metal hyperaccumulation, edaphic adaptation, extremophile, Brassicaceae, meiosis, transposable element, LTR-TE

Introduction

Heavy metals, such as zinc (Zn), cadmium (Cd) and lead (Pb), are naturally omnipresent in the biosphere at very low levels. Their concentrations can be regionally elevated and are extremely high locally at rare sites as a result of geological anomalies. Human activities, for example ore mining, metallurgical processing and sewage sludge deposition, contribute to anthropogenic contamination of the biosphere with heavy metals, threatening environmental and human health (Nriagu & Pacyna, 1988; Lamas *et al.*, 2016). Heavy metal-enriched habitats often host characteristic ecological communities, especially where human activities have introduced extremely high, toxic levels of heavy metals only recently after the beginning of the industrial revolution (Ernst, 1974). Here we use comparative transcriptomics to uncover the molecular basis of local adaptation to an extremely highly heavy metal-contaminated soil in a land plant as a complex multi-cellular eukaryotic organism.

The Brassicaceae species *Arabidopsis halleri*, in the sister clade of the genetic model plant *Arabidopsis thaliana*, is an emerging perennial model plant (Krämer, 2015; Honjo & Kudoh, 2019; Nagano *et al.*, 2019). *A. halleri*, a perennial stoloniferous obligate outcrosser, has repeatedly colonized highly heavy metal-contaminated, so-called metalliferous (M) soils (Ernst, 1974; Bert *et al.*, 2000; Stein *et al.*, 2017). Natural populations of *A. halleri* are also found on non-contaminated (non-metalliferous, NM) soils. Irrespective of its habitat soil type, *A. halleri* is a Zn and Cd hyperaccumulator (Ernst, 1974; Bert *et al.*, 2000; Stein *et al.*, 2017). The about 750 known hyperaccumulator plant species are land plants of which at least one individual was identified to accumulate a metal or metalloid in its above-ground tissues to concentrations more than one order of magnitude above critical toxicity thresholds of ordinary plants, at its natural site of growth in the field (Reeves *et al.*, 2018). Hyperaccumulation in plants can act as an elemental defense against biotic stress (Kazemi-Dinan *et al.*, 2014), and the associated species-wide heavy metal tolerance can apparently facilitate the colonization of M soils by *A. halleri* (Pauwels *et al.*, 2005; Meyer *et al.*, 2010).

Cross-species comparative transcriptomics studies of *A. halleri* and *A. thaliana* established tens of candidate metal homeostasis genes for roles in metal hyperaccumulation or metal hypertolerance, which encode various transmembrane transporters of metal cations and isoforms of a metal chelator biosynthetic enzyme (Becher *et al.*, 2004; Weber *et al.*, 2004; Talke *et al.*, 2006). Although the generation of transgenic plants remains technically demanding and time-consuming in *A. halleri*, subsequent work demonstrated functions in metal hyperaccumulation or hypertolerance for some of these genes. The key locus making the largest known contribution to both metal hyperaccumulation and hypertolerance in *A. halleri* is *Heavy Metal ATPase 4* (*HMA4*), which encodes a plasma membrane P_{1B}-type metal ATPase mediating cellular export for xylem loading of Zn and Cd in the root (Talke *et al.*, 2006; Hanikenne *et al.*, 2008). Transcript levels of *HMA4* are substantially higher

in *A. halleri* than in *A. thaliana* independently of cultivation conditions, as was also observed for tens of other candidate genes. A combination of modified *cis*-regulation and gene copy number expansion accounts for high expression of *HMA4* (Hanikenne *et al.*, 2008). Examples of other candidate genes with experimentally demonstrated functions in *A. halleri* include *NICOTIANAMINE SYNTHASE 2* (*NAS2*) (Deinlein *et al.*, 2012) contributing to Zn hyperaccumulation, *METAL TRANSPORT PROTEIN1* (*MTP1*) acting in Zn tolerance (Dräger *et al.*, 2004) and Ca^{2+}/H^{+} *exchanger 1* (*CAX1*) functioning to enhance Cd tolerance (Baliardini *et al.*, 2015). While metal hyperaccumulation and hypertolerance are species-wide traits in *A. halleri*, there is additionally a large extent of within-species variation in the levels of metal accumulation, metal tolerance and gene expression (Meyer *et al.*, 2015; Stein *et al.*, 2017; Corso *et al.*, 2018; Schvartzman *et al.*, 2018).

Within-species transcriptomic differences between *A. halleri* populations originating from M and NM soils can provide insights into the molecular and physiological alterations associated with the natural colonization of M soils, but they have remained unexplored thus far. In order to address local adaptation to M soil in *A. halleri*, we focused here on the population at the most highly heavy metal-contaminated *A. halleri* site in Europe at Ponte Nossa (Noss/IT) according to a large-scale field survey of 165 European populations (Stein *et al.*, 2017). Noss individuals were more Cd-tolerant and accumulated lower levels of Cd than both closely related *A. halleri* from a population on NM soil in the vicinity, Paisco Loveno (Pais), and more distantly related *A. halleri* from Wallenfels (Wall) on NM soil in Germany. Further contrasting with the less Cd-tolerant plants of NM soil origin, transcriptomic Cd responses including the activation of Fe deficiency responses were attenuated in the highly Cd-tolerant population. Instead, a large number of transcripts differed in abundance in Noss (M soil origin) from both Pais and Wall plants (NM soil origins) irrespective of cultivation conditions. Overrepresentation analysis indicated that differences comprised primarily the global activation of meiosis- and genome integrity maintenance-related functions in somatic tissues of Noss, accompanied by pronouncedly altered levels of few metal homeostasis transcripts known for central roles in Cd accumulation and basal Cd tolerance of *A. thaliana*. Our results suggest the possibility of roles in somatic tissues of *A. halleri* (Noss) for some genes functions known to operate in meiosis of *A. thaliana*. This work provides insights into how land plants cope with rapid anthropogenic environmental change and extreme abiotic stress levels.

Materials and Methods

Plant material and growth conditions

Cuttings were made of *A. halleri* ssp. *halleri* O'Kane & Al-Shehbaz individuals originating from the field (Stein *et al.*, 2017), followed by hydroponic pre-cultivation for 4 weeks to obtain rooted vegetative clones. Experiments were conducted in 1x modified Hoagland's solution (Becher *et al.*,

71 2004) with weekly exchange of solutions. In Cd tolerance assays, plants were sequentially exposed
72 to step-wise increasing concentrations of $CdSO_4$ (0, 25, 50, 75, 100, 125, 150, 175, 200, 250, 300,
73 350, 400 and 450 µM) once per week in a growth chamber (10-h light at 90 µmol photons m^{-2} s^{-1},
74 22°C/ 14-h dark at 18°C, 65% constant relative humidity). Cd tolerance index was quantified as
75 EC_{100}, the effective Cd concentration causing 100% root growth inhibition (Schat & Ten Bookum,
76 1992). For transcriptome sequencing and multi-element analysis (Table S4), 1x modified Hoagland's
77 solution was supplemented with either 2 or 0 (control) µM $CdSO_4$, with cultivation in 16-h light (90
78 µmol photons m^{-2} s^{-1}, 22°C)/ 8-h dark (18°C) cycles at 60% constant relative humidity for 16 d.

79 **Multi-element analysis and transcriptome sequencing**

80 For multi-element analysis, apoplastically bound metal cations were desorbed from freshly harvested
81 roots (Cailliatte *et al.*, 2010). All tissues were washed twice in ddH_2O before drying, digestion and
82 multi-element analysis as described (Stein *et al.*, 2017). For transcriptome sequencing, root and shoot
83 tissues were harvested separately 7 h after the onset of the light period, frozen immediately in liquid
84 nitrogen, pooled from six replicate clones per genotype, treatment and experiment, and stored at -
85 80°C. Total RNA was extracted from aliquots of tissue homogenates using the RNeasy Plant Mini
86 Kit (Qiagen, Hilden, Germany). One µg of total RNA was used in NEBNext Ultra II RNA Library
87 Prep Kit for Illumina (New England Biolabs, Frankfurt, Germany), followed by sequencing to obtain
88 14 to 29 mio. 150-bp read pairs per sample that passed quality filters (Novogene, Hongkong).

89 **Sequence data analysis**

90 Reads were mapped to the *A. halleri* ssp. *gemmifera* (Matsumura) O'Kane & Al-Shehbaz accession
91 Tada mine (W302) reference genome (Briskine *et al.*, 2017) using HISAT2 version 2.1.0 (Kim *et al.*,
92 2015). This reference genome contains a more complete set of *A. halleri* coding regions than the *A.*
93 *lyrata* reference genome, and its use resulted in considerably higher mapping rates. After multiple
94 mapping error correction according to COMEX 2.1 (Pietzenuk *et al.*, 2016), the number of fragments
95 per gene were determined using Qualimap2 (Okonechnikov *et al.*, 2016), followed by principal
96 component analysis (PCA) and differential gene expression analysis using the R package *DESeq2*
97 (Love *et al.*, 2014). Clustering was performed using the R package *pheatmap*. For gene ontology
98 (GO) term enrichment analyses *A. halleri* gene IDs were converted into *A. thaliana* TAIR10 AGI
99 codes, which were then used in hypergeometric distribution estimation through the function g:GOSt
100 built in g:Profiler (Reimand *et al.*, 2016). TE transcript levels were quantified based on Reads Per
101 Kilobase per Million reads (Mortazavi *et al.*, 2008) after mapping to the *Arabidopsis lyrata* MN47
102 reference genome with TE annotations (Pietzenuk *et al.*, 2016). This was necessary because the *A.*
103 *halleri* ssp. *gemmifera* reference genome lacks contiguity outside coding sequences and in repetitive
104 regions and its TE annotations are less thoroughly curated. Reads were used to reconstruct cDNA
105 variants with Integrated Genome Viewer (Robinson *et al.*, 2017). Multiple comparisons of means

106 were conducted using the *stats* and *agricolae*, with normality and homoscedasticity tests in the *car*,
107 packages in R (R_Core_Team, 2013).

108 **Validation by RT-qPCR and immunoblots**

109 We used aliquots of homogenized tissues as frozen during harvest. Real-time RT-qPCR reactions
110 were run in a 384-well LightCycler®480 II System (Roche Diagnostics, Mannheim, Germany) using
111 the GoTaq qPCR Mastermix (Promega, Walldorf, Germany) and cDNAs synthesized from DNase-
112 treated total RNA using the RevertAid First Strand cDNA Synthesis Kit (Thermo Fisher Scientific,
113 Schwerte, Germany). Immunoblots were carried out following SDS-PAGE (Lämmli, 1970) using
114 anti-*At*IRT1 (AS11 1780, Lot number 1203; Agrisera, Vännas, Sweden), HRP-conjugated secondary
115 antibodies (Thermo Fisher Scientific) and detection using the ECL Select Western Blotting Detection
116 Reagent (GE Healthcare, Little Chalfont, England) and a Fusion Fx7 GelDoc (Vilber Lourmat,
117 Eberhardzell, Germany).

118

119 **Results**

120 **Choice of populations and comparative physiological characterization**

121 In a field survey of 165 *Arabidopsis halleri* sites across Europe, average soil Cd concentrations were
122 by far the highest at Ponte Nossa/IT (Noss) in both the total and hydrochloric acid-extractable soil
123 fractions (900 and 203 mg Cd kg^{-1} soil, respectively; second highest were soils of far lower
124 concentrations of 130 and 87 mg Cd kg^{-1} soil, respectively)(Stein *et al.*, 2017). Therefore, we chose
125 the *A. halleri* population at this M site as the focal population in this comparative study, in
126 combination with two populations at NM sites for comparison, one from the geographically closest
127 site near Paisco Loveno (Pais/IT) approximately 38 km northeast of Noss, and one near Wallenfels
128 (Wall/DE) about 520 km to the North. Average soil total Cd concentrations in close proximity of the
129 *A. halleri* individuals studied here were 700-fold higher at Noss than at Pais (Table S1). Previously
130 published comparative transcriptomics studies of Zn/Cd hyperaccumulator plant species included
131 individuals originating from geographically distant M sites only, for example in Italy and Poland for
132 *A. halleri*, and they were not designed to compare between M and NM sites (Corso *et al.*, 2018;
133 Schvartzman *et al.*, 2018; Halimaa *et al.*, 2019).

134 In order to test for local adaptation of the Noss population to high soil Cd levels, we quantified Cd
135 tolerance of individuals collected at each of the three sites in hydroponic culture system in a growth
136 chamber. Based on the proportion of individuals maintaining root growth in a sequential exposure
137 test with stepwise increasing Cd concentrations, Noss was the most tolerant (Fig. 1a, Table S2, Fig.
138 S1). Following a different approach for quantifying metal tolerance (Schat & Ten Bookum, 1992),
139 mean EC_{100}, the effective Cd concentration causing 100% root growth inhibition in a given

140 individual, was significantly higher for Noss (344 ± 98 μM Cd) than for Pais (219 ± 66 μM Cd) and
141 Wall (221 ± 56 μM Cd) (Fig. 1b).
142 In natural populations in the field, Cd concentrations accumulated in leaves of *A. halleri* at Noss were
143 at least 20-fold higher than at Pais and 3-fold higher than at Wall (Table S1)(Stein *et al.*, 2017). By
144 contrast, Zn concentrations in leaves of field-collected individuals were similar in all three
145 populations, despite vastly differing soil Zn levels. The leaf:soil ratio of Cd concentrations (Cd
146 accumulation efficiency) in the field was highest in the Wall population from north of the Alps and
147 lowest in Noss, suggesting attenuated leaf Cd accumulation at Noss compared to both Pais and Wall
148 (Fig. 1c). Upon exposure to a sub-toxic concentration of 2 μM $CdSO_4$ in hydroponic culture for 16
149 d, Cd concentrations in roots of Noss (140 ± 74 μg Cd g^{-1} DW) were only 43% and 40% of those in
150 Pais and Wall, respectively (Fig. 1d, Table S3). Leaf Cd concentrations were also lower in Noss (160
151 ± 74 μg Cd g^{-1} DW) than in Wall (about 52% of Wall; $P < 0.05$), and at about 76% of those in Pais
152 (n.s.). We additionally observed between-population differences in the accumulation of other
153 nutrients (Fig. S2). Upon Cd exposure, Cu concentrations were higher, and Mn concentrations were
154 lower than under control conditions in roots of Pais and Wall, but not in roots of Noss (Fig. S2a and
155 D). Fe concentrations were higher in roots of Noss and increased further following exposure to Cd,
156 in contrast to the two populations from NM soils (Fig. S2e). In shoots of Noss, Fe concentrations
157 were about twice as high (*ca*. 75 μg Fe g^{-1} DW) than in the shoots of the other two populations under
158 both control and Cd exposure conditions (Fig. S2e). Taken together, these results showed that the
159 Noss population of *A. halleri* is more tolerant to Cd than both Pais and Wall, supporting adaptation
160 to local soil. This was accompanied by attenuated Cd accumulation and a distinct profile of tissue
161 concentrations of micronutrient metals in Noss under standardized growth conditions in hydroponic
162 culture.
163
164 **Comparative transcriptomics**
165 Transcriptome sequencing was carried out for a total of 72 samples, with three independent repeats
166 of each experiment comprising root and shoot tissues of two genotypes from each of the three
167 populations grown in control and Cd-amended medium for 16 d (0 and 2 μM $CdSO_4$; Table S4; note
168 that this Cd concentration is far sub-toxic in all *A. halleri* populations under investigation). Principal
169 component analysis (PCA) suggested predominant differences between root and shoot
170 transcriptomes (Fig. S3a). In both roots and shoots, transcriptomes of the geographically neighboring
171 populations Noss and Pais grouped closer together in the first principal component by comparison to
172 the geographically distant Wall population (Fig. S3b and c). This suggested that individuals from
173 Noss and Pais are genetically more closely related to one another than either of these to individuals
174 from Wall. Based on gentyping-by-sequencing of more than 800 European *A. halleri* individuals, we

175 established that Noss and Pais are both in the Central Alpine clade of *A. halleri*, whereas Wall is in
176 the distinct Central European clade (Anderson *et al*., manuscript in preparation).
177 Upon long-term exposure to a low level of Cd as applied here, transcriptomic differences compared
178 to controls untreated with Cd comprised a few hundred genes in both the Pais and the Wall population
179 originating from NM sites (Fig. 2a and b, Figs. S4 and S5, Dataset S1). By contrast, in the more Cd-
180 tolerant population Noss, no single transcript responded in abundance to Cd exposure under the
181 employed conditions in either roots or shoots. This observation is relevant because it argues against
182 the possible hypothesis that adaptation of *A. halleri* to high-Cd soils involves an enhanced sensitivity
183 of transcriptional responsiveness to Cd. In order to identify candidate transcripts that may contribute
184 to the ability of the Noss population to persist on extremely highly heavy metal-contaminated soil,
185 we next examined the genes showing differential expression between populations (Fig. 2c and d,
186 Dataset S2). As an initial set of candidate genes, we focused on those transcripts showing differential
187 abundance between Noss (M) and both of the populations from NM soils, Pais and Wall. This
188 comparison identified differential transcript levels for as many as 1,617 genes (801/599/217, higher
189 in Noss/ lower in Noss / intermediate in Noss) in roots and 1,638 genes (797/604/237) in shoots under
190 control conditions (under Cd exposure 848/697/236 and 1140/707/339 in roots and shoots,
191 respectively) (surrounded by a red line in Fig. 2c and d).
192
193 **Candidate genes differentially expressed in Noss**
194 We subjected the genes expressed either at higher or lower levels in Noss compared to both Pais and
195 Wall (DEGs; 0 µM Cd; Dataset S3) to a Gene Ontology Term (GO) enrichment analysis (Dataset
196 S4). Meiotic cell cycle (GO:0051321) was the most significantly enriched in the group of genes that
197 are more highly expressed in both root and shoot of Noss (Fig. 3a and b, Table 1). Among the genes
198 within the GO term meiotic cell cycle, transcript levels of *ARGONAUTE 9* (*AGO9*) were substantially
199 higher in both root and shoot tissues of the Noss in comparison to both the Pais and Wall populations
200 (Fig. 3c and d, Table S5; Log_2FC = 6.6 and 4.4 to 4.6 in root and shoot, respectively; see Dataset S2).
201 By contrast, present knowledge suggests that the expression of *AGO9* in *A. thaliana* is restricted to
202 only a few cells during the early stages of meiotic megaspore formation (Duran-Figueroa & Vielle-
203 Calzada, 2010; Olmedo-Monfil *et al.*, 2010). Amino acid sequence alignment of AGO proteins in *A.*
204 *halleri* and *A. thaliana* (Fig. S6) confirmed that *Ah*AGO9 is the closest *A. halleri* homologue of
205 *At*AGO9 in clade 3 of ARGONAUTE proteins (AGO4, -6, -8 and -9)(Vaucheret, 2008). Sequence
206 read coverage for *AGO9*, obtained from gDNA of Noss and Pais, suggested that *AGO9* is a single-
207 copy gene (Table S6).
208 In the GO class meiotic cell cycle, transcript levels of the two gene copies of *ZIPper I* (*ZYP1a* and
209 *ZYP1b*) were also substantially higher in Noss than in both Pais and Wall (Fig. 3e and f, Tables S5

210 and S6). Amino acid sequences of *At*ZYP1a and b are highly similar and conserved in *Ah*ZYP1a and
211 b (Fig. S7). We validated sequencing-based transcriptomic data by reverse-transcription quantitative
212 real-time PCR for a representative set of genes including *AGO9* and *ZYP1a/b* (Table S8, Fig. S9).
213 An additional 15 genes in roots and 10 genes in shoots of the GO meiotic cell cycle showed elevated
214 transcript levels in Noss compared to both populations of NM soil (see Fig. 3a and b, Dataset S4).
215 The partly overlapping categories homologous recombination (GO:0035825), reciprocal meiotic
216 recombination (GO:0007131), meiosis I cell cycle process (GO:0061982) and condensed
217 chromosome (GO:0000793) were also enriched among transcripts of increased abundance in roots
218 of Noss. Among a total of 23 genes that were more highly expressed in either roots or shoots of Noss
219 compared to both Pais and Wall as well as grouped in over-represented GO terms related to meiotic
220 cell cycle and homologous/meiotic recombination, homologs of eight genes (35%) were previously
221 shown to have roles or implicated in somatic DNA repair in *A. thaliana* (Table 1). Furthermore, sulfur
222 compound metabolic process (GO:0006790), glucosinolate biosynthetic process (GO:0019761) and
223 plastid (GO:0009536) were enriched among transcripts of decreased abundance in shoot tissues of
224 Noss (see Dataset S4).
225
226 **Differential abundance of metal homeostasis-related transcripts between populations**
227 Next, we sought to identify metal homeostasis candidate genes contributing to the observed
228 differences in Cd tolerance and accumulation between Noss and the two other populations. For this
229 purpose, we intersected a manually curated list of metal homeostasis genes with the list of candidate
230 transcripts (see Fig. 2e-g, $|Log_2FC| > 1$, mean normalized counts across all samples > 2; Dataset S3,
231 Table S7). Transcript levels of *Heavy Metal ATPase 2* (*HMA2*) and two *ZRT/IRT-like Protein* genes,
232 *ZIP2* and *ZIP6*, were higher in roots of Noss than Pais and Wall (Fig. 3e). Root transcript levels of
233 *Iron-Regulated Transporter 1* (*IRT1*), *Plant Cadmium Resistance 9* (*PCR9*) and *ZIP10* were lower
234 in Noss (Fig. 3f). In shoots of Noss, transcript levels of *PCR8*, *HMA2* and *Cation/H*$^+$ *Exchanger 2*
235 (*CHX2*) were higher than in both Pais and Wall (Fig. 3g).
236 The IRT1 transmembrane transport protein is known as the high-affinity root iron (Fe^{2+}) uptake
237 system of dicotyledonous plants as well as the predominating path for inadvertent uptake of Cd^{2+} in
238 Arabidopsis (Vert *et al.*, 2002). Compared to Pais and Wall, an 84% to 92% lower expression of *IRT1*
239 in Noss (see Fig. 3f) would provide an intuitive adaptive route towards plant Cd tolerance *via*
240 exclusion (see Fig. 1d, Fig. S8). In *A. thaliana*, *IRT1* expression is under complex regulation at both
241 the transcriptional and post-transcriptional levels (Kerkeb *et al.*, 2008). To test whether reduced IRT1
242 protein levels accompany low *IRT1* transcript abundance in Noss, we carried out immunoblot
243 detection using an anti-*At*IRT1 antibody in subsamples of root tissues from the same experiments.
244 At the size corresponding to IRT1 of Fe-deficient *A. thaliana* (Fig. 3h, right lane), we observed weak

245 bands in both Pais and Wall cultivated under both control and 2 µM Cd exposure conditions, but no
246 band was visible in Noss, in agreement with our observations at the transcript level. Additional bands
247 observed in *A. halleri* at higher molecular masses are likely to constitute non-specific cross-reactions
248 of the antibody (44 kDa). The sizes of bands at approximately 48 and 56 kDa are also consistent with
249 multiply ubiquitinated forms of IRT1, respectively, previously reported at distances of multiples of
250 ~9 kDa from IRT1 (Fig. 3h)(Barberon *et al.*, 2011; Callis, 2014). In *A. thaliana*, the ubiquitination
251 of IRT1 leads to its deactivation by removal from the plasma membrane through endocytosis
252 (Barberon *et al.*, 2011). Taking these data together, the absence of a signal corresponding to the size
253 of functional IRT1 in Noss on immunoblots was in agreement with the between-population
254 differences observed for *IRT1* transcript levels using RNA-seq and RT-qPCR.
255
256 **Cd exposure elicits transcriptional Fe deficiency responses in both populations from NM sites**
257 In the less Cd-tolerant populations, upon exposure to Cd, we found differential transcript abundance
258 for 210 genes (upregulated 53, downregulated 157) in shoots and of 428 genes (upregulated 143,
259 downregulated 285) in roots of Pais. A similar number of 197 (upregulated 65, downregulated 132)
260 in roots and 243 (upregulated 98, downregulated 145) in shoots responded to Cd in Wall (see Fig. 2a
261 and b, Dataset S5). Of these, the responses of 44 genes in roots and of 84 genes in shoots were shared
262 between both populations from NM soil, a larger number than expected by chance ($P < 10^{-50}$,
263 hypergeometric test). Transcriptomic Cd responses of both Pais and Wall were enriched in Fe
264 deficiency responses (Fig. 4, Dataset S6). The associated enriched GO categories included cellular
265 response to iron ion starvation (GO:0010106) among the upregulated transcripts, as well as
266 intracellular sequestering of iron ion (GO:0006880) and ferroxidase activity (GO:0004322) among
267 the downregulated transcripts in both roots and shoots.
268 Among transcripts known to increase in abundance in *A. thaliana* under iron deficiency, transcript
269 levels of *Popeye* (*PYE*), *Basic Helix-Loop-Helix 38/39/100/101* (*bHLH38/39/100/101*) transcription
270 factors, *Brutus* (*BTS*) and *Brutus-like 1* (*BTSL1*), as well as *Ferric Reduction Oxidases* (*FRO1* and
271 *FRO3*), *Nicotianamine Synthase 4* (*NAS4*), *Zinc Induced Facilitator 1* (*ZIF1*), *Oligopeptide*
272 *Transporter 3* (*OPT3*) and *Natural Resistance-Associated Macrophage Protein 3* (*NRAMP3*)
273 increased under Cd exposure (Table S9a). A number of genes have roles in iron storage/sequestration,
274 and their transcript levels are downregulated under iron deficiency in *A. thaliana*. Of these, *Ferritin*
275 (*FER1*, *FER3* and *FER4*) and *Vacuolar iron Transporter-Like protein* (*VTL1* and *VTL5*) transcript
276 levels were downregulated in Cd-exposed Pais and Wall plants (Table S9b).
277 Further GOs enriched among transcripts downregulated in abundance in response to Cd were
278 response to reactive oxygen species (GO:0000302), photosynthesis (GO:0015979), and chloroplast
279 thylakoid membrane (GO:0009535). The gene content of these, however, is less compelling in

implicating the respective biological processes (see Table S9b; Datasets S5 and S6). Chloroplast thylakoid membrane is a child term of plastid (GO:0009536), which was enriched among transcripts present at lower levels in Noss than in both Pais and Wall. Six genes were in common between these (Table S10), of which only one, *Light Harvesting Complex of photosystem II* (*LHCB4.2*), appears to function directly in photosynthesis. A more extensive search for transcripts that are Cd-responsive in both Pais and Wall as well as differentially expressed in the Noss population identified *Bifunctional inhibitor/lipid-transfer protein/seed storage 2S albumin superfamily protein* in the root and *NAD(P)-binding Rossmann-fold superfamily protein* in the shoot (Table S11). Finally, metal homeostasis protein-encoding transcripts upregulated in abundance upon Cd exposure in Pais or Wall were generally less abundant in Noss regardless of Cd treatment (Fig. S10, cluster R5 and S5). Conversely, metal homeostasis protein-coding transcripts that were decreased in abundance under Cd exposure in Pais or Wall were generally present at higher levels in Noss (Fig. S10, cluster R2 and S2). These between-population differences primarily comprised genes associated with Fe deficiency responses of *A. thaliana* as described above (see Fig. 4, Table S9), thus indicating against a constitutive proactive activation in more Cd-tolerant Noss of the transcriptional Cd responses observed here in the less Cd-tolerant Pais and Wall populations. These results suggested that transcriptional symptoms elicited by Cd exposure were observed already at far-subtoxic Cd concentrations, which neither caused growth impairment nor chlorosis, in the two less Cd-tolerant populations originating from NM soils.

Lower transcript levels of long terminal repeat retrotransposons in Noss

Comparative transcriptomics suggested that in particular, *AGO9* transcript levels were higher in Noss compared to both Pais and Wall (see Fig. 3c and d). If this were indeed the case, then we would expect that long terminal repeat retrotransposons (LTR-TEs), target loci known to be transcriptionally silenced dependent on *AGO9* in *A. thaliana*, are less transcriptionally active in *A. halleri* from Noss than *A. halleri* from Pais and Wall (Duran-Figueroa & Vielle-Calzada, 2010). In Noss, transcript levels derived from LTR-TEs were lower in shoot tissues by comparison to both Pais and Wall and also lower in root tissues than in Pais (Fig. 5, Fig. S11, Dataset S7).

Elevated *AGO9* transcript levels in *A. halleri* originating from European M sites

We identified two additional pairs of one *A. halleri* population at a highly metal-contaminated (M) site and one at a non-contaminated (NM) site in a common geographic region in Poland and Germany, respectively (Stein *et al.*, 2017), all belonging to the Central European clade (Anderson *et al.*, manuscript in preparation). Individuals originating from these sites were cultivated hydroponically alongside the individuals of this study. Quantification of *AGO9* transcript levels by RT-qPCR

independently confirmed higher transcript levels in *A. halleri* individuals from Noss compared to Pais (Fig. 6; see Fig. 3d, Dataset S2). Moreover, *AGO9* transcript levels were higher in *A. halleri* individuals from Polish and German M sites, Miasteczko Śląskie (Mias/PL) and Lautenthal (Laut/DE), compared to their respective NM site counterparts, Zakopane (Zapa/PL) and Wallenfels (Wall/DE). This finding suggests that, compared to neighbouring NM sites, elevated expression of *AGO9* is common among individuals from M site populations in several regions of Europe, even where soil heavy metal levels were far lower than at the extreme site Noss.

Discussion

Divergent transcript levels between populations arise more abundantly than divergent transcriptomic responses to Cd

To globally identify molecular alterations associated with plant adaptation to extreme abiotic stress, we conducted comparative transcriptomics of *A. halleri* populations from contrasting environments of origin (Fig. 2). In line with their origin from the most highly Cd-contaminated *A. halleri* site known in Europe, our results support environment-dependent phenotypic differentiation in *A. halleri* and adaptation to high soil Cd levels at Noss (Fig. 1). Transcript levels of a few hundred genes differed between Cd-exposed and unexposed *A. halleri* plants from the two populations originating from NM soils, Pais and Wall. Thus, these less Cd-tolerant plants attained a different transcriptomic state in the presence of Cd through a process that must involve the initial interaction of Cd^{2+} with primary Cd-sensing or -sensitive sites, of which the molecular identities are yet unknown. By contrast, in *A. halleri* from the more Cd-tolerant Noss (M) population, there was no single gene of which transcript levels differed between the Cd and the control treatment (Fig. 2). This implies that in Noss, Cd^{2+} was either effectively kept away from all Cd-sensing and -sensitive sites (Krämer, 2018), which is likely, or alternatively Cd^{2+} did not result in any transcriptomic adjustment within a timeframe relevant for our harvest after 16 d of exposure. Given that Noss is more Cd-tolerant than both Pais and Wall (see Fig. 1), the molecular mechanisms conferring tolerance must then either be active also in the absence of Cd, or alternatively their implementation must operate entirely downstream of transcript levels, for example at the translational or post-translational level.

Several thousand transcripts differed in abundance between the Noss (M) population of *A. halleri* and either one of the two populations originating from NM sites irrespective of Cd exposure (Fig. 2; see also Fig. S10). This suggests that between-population transcriptomic divergence is substantial even among the geographically proximal and phylogenetically closely related *A. halleri* populations Noss and Pais (Figs. S3, S11; Anderson *et al*., manuscript in preparation), by comparison to between-population differences in the responses to Cd exposure. Similarly, earlier cross-species comparative transcriptomics studies identified responses to metal exposure in *A. thaliana*, a species with only

350 basal metal tolerance, whereas there were no remarkable additional species-specific responses among
351 metal homeostasis genes in the metal-hypertolerant species *A. halleri* (Talke *et al.*, 2006; Weber *et*
352 *al.*, 2006). Instead, tens of genes with predicted roles in metal homeostasis were more highly
353 expressed in *A. halleri* compared to *A. thaliana* irrespective of the growth conditions.
354
355 **Constitutive global activation of meiosis-related genes**
356 Meiosis is essential for sexual reproduction in eukaryotes and occurs exclusively in male and female
357 gametophyte precursor cells during the reproductive phase of the life cycle (Mercier *et al.*, 2015).
358 Yet, in somatic tissues we observed an overrepresentation of the Gene Ontology Term (GO) "meiotic
359 cell cycle" among transcripts of higher abundance in Noss by comparison to both Pais and Wall (Fig.
360 3, Table 1, Dataset S4). This included genes functioning during entry into meiosis (*AGO9*, *SWI1*),
361 cohesion complex (*SMC3*), synaptonemal complex (*ZYP1a/b*), recombination and its control (*PRD3*,
362 *BRCA2B*, *MHF2*, *MSH5*, *FLIP*), for example, in *A. thaliana* (Mercier *et al.*, 2015). In addition to its
363 role during meiosis, DNA double-strand break repair (DSBR) through homologous recombination
364 (HR) functions to maintain genome integrity following DNA damage in somatic cells (Schuermann
365 *et al.*, 2005). Exposure of plants to an excess of aluminum, boron or heavy metal ions can cause DNA
366 damage (Kovalchuk *et al.*, 2001; Rounds & Larsen, 2008; Sakamoto *et al.*, 2011; Morales *et al.*,
367 2016). Of the meiosis-related genes identified here, there is evidence for an additional involvement
368 in somatic HR-mediated DSBR for *BRCA2* (Seeliger *et al.*, 2012), *EME1A/B* (Geuting *et al.*, 2009),
369 *HEB2* (Sakamoto *et al.*, 2011), *FLIP* (Bouyer *et al.*, 2018; Fernandes *et al.*, 2018), *RPA2B* (Liu *et*
370 *al.*, 2017) and *ERCC1* (Dubest *et al.*, 2004) in *A. thaliana* (Table 1; Dataset S4). *ERCC1* was also
371 implicated in non-HR nucleotide excision repair (Hefner *et al.*, 2003).
372 The two most strongly differentially expressed meiosis-related genes, *AGO9* and *ZYP1a/b*, were so
373 far thought to function exclusively in reproductive development of *A. thaliana*. *AGO9* is required
374 pre-meiotically to prevent the formation of excessive gametophytic precursor cells and expressed in
375 a single layer of somatic companion cells surrounding the megaspore mother cell, as well as in pollen
376 in *A. thaliana* (Olmedo-Monfil *et al.*, 2010). *At*AGO9 was proposed to act in the silencing of
377 pericentromeric TEs, predominantly long terminal repeat retrotransposons (LTR-TEs), in the ovule
378 through the interaction with 24-nucleotide small RNAs (Duran-Figueroa & Vielle-Calzada, 2010).
379 Like other organisms, plants generally inactivate TEs in order to maintain genomic stability.
380 Exposure to abiotic stress, including also heavy metal exposure, can result in the expression and
381 transposition of some TEs, especially LTR-TEs, in plants (Grandbastien, 2015) and other organisms
382 (Horvath *et al.*, 2017). In *A. halleri* from Noss elevated expression of *AGO9* in somatic cells may
383 serve to counteract LTR-TE activation as an adaptation to their high-stress natural environment.

384 Consistent with this hypothesis, transcripts derived from LTR-TEs were present at overall lower
385 levels in both root and shoot tissues of Noss compared to Pais (Fig. 5).
386 We detected no global increase in the levels of transcripts derived from LTR-TEs or any other TEs
387 at 2 µM Cd compared to control conditions. It is possible that an increase in TE expression is locus-
388 specific, or occurs at different times after the onset of Cd exposure or at higher levels of Cd exposure
389 which plants might encounter at the Noss site at least temporarily (Krämer, 2018), or in response to
390 other abiotic stresses or combined stress exposure, in nature (see Table S1). Published circumstantial
391 evidence has implicated *AGO9* in DNA damage repair in seedlings of *A. thaliana*, i.e. at the
392 vegetative stage (Oliver *et al.*, 2014). Available antibodies against *A. thaliana* AGO9 and ZYP1 did
393 not detect specific bands in immunoblots of floral buds in our hands, as established by comparing
394 wild-type Arabidopsis with the corresponding mutants (data not shown). Future work will address
395 the biological functions of *AGO9* in somatic tissues of *A. halleri*.
396 We propose that our results reflect a constitutive transcriptional activation of genome integrity
397 maintenance in vegetative tissues as a component of extreme abiotic stress adaptation of *A. halleri* at
398 Noss. The genes newly implicated here in somatic genome integrity maintenance (Table 1) may have
399 remained unidentified in the past because their functions in somatic cells are specific to *A. halleri* or
400 because extremely low general expression levels may be sufficient to accomplish a possible somatic
401 DNA repair function in *A. thaliana*. It should be noted that Cd is not the only abiotic stress factor at
402 the Noss site in the field, where soil concentrations of Zn, Pb and Cu are also extremely high (Stein
403 *et al.*, 2017).
404 Of the meiosis genes showing elevated transcript levels in *A. halleri* from Noss (see Table 1), the
405 four genes *ZYP1a/b*, *PRD3* and *SMC3* were among a total of eight meiosis genes identified to be
406 under selection in autotetraploid *Arabidopsis arenosa*, for which there is no information on transcript
407 levels to date (Yant *et al.*, 2013). The predicted amino acid substitutions reported as hallmarks of
408 tetraploidy in *A. arenosa*, when also divergent from diploid *A. thaliana* (Col), were all absent in *A.*
409 *halleri* individuals from both Noss and Pais (data not shown). Moreover, all known *A. halleri* are
410 diploid, including all populations of this study (Anderson *et al.*, manuscript in preparation). We
411 conclude that the alterations in meiosis gene expression in plants adapted to an extreme environment
412 reported here are unrelated to published work on the adaptation of meiosis to tetraploidy that was
413 initially conducted in *A. arenosa* (Bomblies *et al.*, 2015).
414
415 **Large alterations only few metal homeostasis functions in *A. halleri* from Noss**
416 Attenuated Cd accumulation in *A. halleri* from Noss (see Fig. 1) observed here in hydroponics is
417 consistent with earlier results from the cultivation of Noss and Wall on an artificially Cd-
418 contaminated soil (Stein *et al.*, 2017) and with observations in hydroponic culture on accessions

419 collected nearby (Meyer *et al.*, 2015; Corso *et al.*, 2018). Among metal homeostasis genes, we
420 observed substantially lower *IRT1* expression in roots of Noss compared to both Pais and Wall at
421 both the transcript (Fig. 3f) and protein levels (Fig. 3h). This can account for both enhanced Cd
422 hypertolerance and attenuated Cd accumulation in *A. halleri* from Noss when extrapolating from *A.*
423 *thaliana irt1* mutants (Vert *et al.*, 2002). Taking our data together, comparably high tissue levels of
424 iron (Fig. S1) in Noss plants appear to arise independently of IRT1 (Fig. 3h), which warrants further
425 study.
426 Distinctly higher transcript levels of *HMA2* in both roots and shoots of Noss (Fig. 3e and g) when
427 compared to both the Pais and the Wall populations suggest that enhanced cellular export of Cd
428 contributes to enhanced Cd hypertolerance in this population. Alongside HMA4, the plasma
429 membrane efflux pump HMA2 mediates root-to-shoot translocation of Zn in *A. thaliana* and can also
430 transport chemically similar Cd^{2+} ions (Hussain *et al.*, 2004). The *HMA2* transcript is present in roots
431 of Zn-deficient *A. thaliana*, in particular (Sinclair *et al.*, 2018). A possible role of *HMA2* in the
432 adaptation of *A. halleri* to local soil composition in Noss must involve functional alterations
433 compared to *A. thaliana*.
434
435 **Cd exposure induces Fe deficiency responses in both populations from NM sites**
436 In the less Cd-tolerant Wall and Pais populations originating from NM soils, we observed Fe
437 deficiency response-like transcriptomic changes upon exposure to 2 µM Cd for 16 d (Fig. 4; Table
438 S9). Plants that are non-hypertolerant to metals, for example *A. thaliana*, activate aspects of Fe
439 deficiency responses when exposed to an excess of heavy metals, for example Cd (Leskova *et al.*,
440 2017). Previously published results in *A. thaliana* were from heavy metal treatment conditions
441 causing a mix of possible toxicity symptoms and acclimation responses. By contrast, in this present
442 study the Cd treatment condition was far below toxicity thresholds of *A. halleri* that is known for
443 species-wide Cd hypertolerance (see Fig. 1). Our data suggest that even under exposure to very low
444 sub-toxic Cd concentrations, transcriptional responses of *A. halleri* reflect symptoms of nutrient
445 imbalances caused by Cd. However, these responses to Cd are not associated with evolutionary
446 adaptation to high-Cd soil in *A. halleri*.
447 A transcriptomics study reported Fe deficiency responses in *A. halleri* from the Polish M site PL22,
448 but not in the I16 population from a metalliferous site close to Noss (M), in response to high-Zn
449 exposure (Schvartzman *et al.*, 2018). A highly Cd-hyperaccumulating accession of *Noccaea*
450 *caerulescens* exhibited a Cd-induced Fe deficiency response, by contrast to a low Cd-accumulating
451 accession (Halimaa *et al.*, 2019). Both of these earlier studies were lacking the comparison with a
452 neighboring population from an NM soil environment that is likely to reflect the most recent
453 environment in evolutionary history, different from the work presented here. Consequently, central

aspects of the heavy metal responses relating to Fe acquisition systems and tissue Fe contents according to this study are novel and cannot be directly compared to earlier studies (Fig. S1, Table S9).

In summary, this comparative study of *A. halleri* populations from different soil types of origin identifies transcriptomic alterations in plants that are adapted to an extreme environment, highly heavy metal-contaminated soil, which has arisen through rapid anthropogenic environmental change.

Acknowledgements

We are grateful to Raphael Mercier (Max Planck Institute for Plant Breeding Research, Cologne, Germany) and Jean-Philippe Vielle-Calzada (CINVESTAV, Mexico City, Mexico) for sharing materials. We thank Petra Düchting, Andreas Aufermann and Jan Riering for assistance (Ruhr University Bochum, Germany). This work was supported by the Deutsche Forschungsgemeinschaft (Research Priority Program SPP1529 ADAPTOMICS, start-up grant to GL/JEA from grant number Kr1967/12 to UK, Research Priority Program SPP1819 RAPID EVOLUTION grant number Kr1967/16 to UK, and individual grant (Kr1967/3-3 to UK); and European Research Council Advanced Grant (grant number 788380 to UK). We acknowledge the Bielefeld-Giessen Center for Microbial Bioinformatics (BiGi) of the German Federal Ministry of Education and Research-funded German network for bioinformatics infrastructure (de.NBI, grant 031A533) for providing computational resources and related general support. Sequence data are available here: PRJEB35573, ENA, EMBL-EBI and MN747968-78 (submission ID: 2287280, Genbank, NCBI).

Author Contribution

Designed research: UK, GL, JQ, JEA, BP; conducted experiments: GL, JQ, HA, VP, LS; analyzed data: GL, UK, JQ, HA, NJ, BP, LS; wrote paper: GL, UK, with contributions from JQ, HA, BP, VP.

Figure Legends

Fig. 1. Cadmium tolerance and accumulation in three populations of *A. halleri*. (a) Proportion of individuals maintaining root growth (elongation) as a function of Cd concentration. Dashed vertical lines indicate ED_{50}, the effective dose required to reach a proportion of 50% according to a dose-response model (see Table S2, Fig. S1). (b) Cd tolerance index. Bars represent mean ± SD of EC_{100} (effective Cd concentration causing 100% root growth inhibition) in a given plant individual (Schat and Ten Bookum, 1992). Plants were sequentially exposed to stepwise increasing concentrations of

489 $CdSO_4$ in hydroponic culture every week (n = 6 to 9 per population, with one to three vegetative
490 clones of each three to six genotypes per population; (a, b)). (c) Cd accumulation efficiency at the
491 site of origin calculated from published field survey data (bars represent means ± SD of n = 11 to 12
492 individuals in the field; units employed, µg Cd g^{-1} dry biomass in leaves, µg total Cd g^{-1} dry mass in
493 soil; data from Stein et al. 2017). (d) Cd concentration in root and shoot tissues of hydroponically
494 cultivated plants. Shown are mean ± SD (n = 12 to 20 clones per population comprising both
495 genotypes, from all three replicate experiments; see Table S1). Four-week-old vegetative clones were
496 exposed to 0 (-Cd) and 2 µM $CdSO_4$ (+Cd) in hydroponic culture for 16 d alongside the plants
497 cultivated for RNA-seq. Different characters denote statistically significant differences between
498 means based on two-way ANOVA, followed by Tukey's HSD test (Log-transformed data were used
499 in (c)) ($P < 0.05$; see Table S3, for nested ANOVA of genotypes within a population (D)).
500
501 **Fig. 2.** Between-population differences according to transcriptome sequencing. (a, b) Venn diagrams
502 show the numbers of genes exhibiting differential transcript abundances under exposure to Cd (+Cd)
503 compared to control conditions (-Cd) for the three populations Noss (N), Pais (P) and Wall (W) in
504 root (a) and shoot (b) tissues. Upregulation (red): Log_2(fold change +Cd *vs*. –Cd) = $Log_2FC > 0.5$;
505 downregulation (blue): $Log_2FC < -0.5$; all with adjusted P-value < 0.05. (c, d) Venn diagrams show
506 the numbers of genes exhibiting differential transcript abundance between populations in root (c) and
507 shoot (d) tissues of plants cultivated under Cd exposure (violet) or control conditions (orange)
508 ($|Log_2FC| > 0.5$; adjusted P-value < 0.05). Red lines surround genes differentially expressed between
509 Noss and both populations of NM soils (Pais and Wall). Four-week-old vegetative clones were
510 exposed to 2 µM Cd or 0 µM Cd (controls) in hydroponic culture for 16 d before harvest. Data are
511 from three independent experiments (repeats), with two genotypes per population and material
512 pooled from six replicate vegetative clones (three hydroponic culture vessels) per genotype in each
513 experiment.
514
515 **Fig. 3.** Candidate genes differentially expressed in Noss compared to both other populations Pais and
516 Wall. (a, b) Significantly enriched gene ontology (GO) categories for roots (a) and shoots (b) of plants
517 cultivated in 0 µM Cd (see Fig. 2c and d, Dataset S3). Genes differentially expressed between Noss
518 from M soil and both Pais and Wall from NM soils were subjected to a GO term enrichment analysis.
519 The number of genes in each over-represented category is shown inside bars (see Dataset S4 for all
520 genes). (c, d) Relative transcript levels of the top three genes (largest between-population differences)
521 taken from (a) and (b) in the over-represented GO category meiotic cell cycle, for roots (c) and shoots
522 (d). (e-g) Relative transcript levels of metal homeostasis genes of which transcript levels are high (e,
523 g) and low (f) in Noss (N) compared to both Pais (P) and Wall (W), for roots (e, f) and shoots (g)

524 (top three genes from Table S7). Bars show means ± SD (n = 6) of normalized counts, which were
525 additionally normalized per kilobase of gene length (NCPK). Different characters represent
526 statistically significant groups based on two-way ANOVA, followed by Tukey's HSD test ($P < 0.05$,
527 see Table S5, for details). Data are from the same experiment as shown in Fig. 2. (h) Immunoblot of
528 IRT1. Total protein extracts (40 µg) from roots of Noss_05, Pais_09 and Wall_07 were separated on
529 a denaturing polyacrylamide gel, blotted, and detection was carried out using an anti-IRT1 antibody.
530 Total protein extract (10 µg) from roots of Fe- and Zn-deficient *A. thaliana* (*Ath*, right lane) served
531 as a positive control, with IRT1 detected as a single band at *ca*. 31 kDa. In *A. halleri*, additional bands
532 at *ca*. 44, 48 and 56 kDa are likely to constitute non-specific ross-reactions of the antibody.
533 Coomassie Blue (CB) stained membrane is shown as a loading control.
534
535 **Fig. 4.** Functional classification of the transcriptional Cd responses in less metal-tolerant populations
536 from NM sites. Significantly enriched GO categories among the transcriptional responses to Cd
537 common in both the Pais and Wall populations for roots (a) and shoots (b) (see Fig. 2a and b, Dataset
538 S6). The numbers of genes in each over-represented category are shown inside bars. Data are from
539 the same experiment as shown in Fig. 2.
540
541 **Fig. 5.** Genome-wide sum of transcript levels contributed by different types of transposable elements
542 in Noss, Pais and Wall. (a-d) Bars show means ± SD (n = 6) of transcript levels of transposable
543 elements (TEs), corresponding to the sum total of RPKM for LTR (Long terminal repeat)
544 retrotransposons (a, b) and non-LTR TEs (c, d) in root (a, c) and shoot (b, d), with RPKM ≥ 7 per
545 locus. Different characters represent statistically significant differences based on one-way ANOVA,
546 followed by Tukey's HSD test ($P < 0.05$).
547
548 **Fig. 6.** *ARGONAUTE 9* (*AGO9*) transcript levels in *A. halleri* individuals originating from
549 metalliferous and non-metalliferous soils in Italy, Poland and Germany. Bargraph shows mean ± SD
550 (n = 4) of relative *AGO9* transcript levels quantified by RT-qPCR in leaves of 5.5-week-old
551 vegetative clones cultivated hydroponically (technical replicates, with two independent PCR runs on
552 each of two independently synthesized cDNAs from a pool of six replicate clones). Data are shown
553 relative to the constitutively expressed gene *Helicase* (*HEL*). Each PCR reaction was conducted in
554 hexuplicate. Different characters represent statistically significant differences based on one-way
555 ANOVA, followed by Tukey's HSD test ($P < 0.05$). For details on collection sites and individuals
556 see Stein et al., 2017.

557

558

559 ## References

560 **Baliardini C, Meyer CL, Salis P, Saumitou-Laprade P, Verbruggen N. 2015.** CATION EXCHANGER1
561 cosegregates with cadmium tolerance in the metal hyperaccumulator *Arabidopsis halleri* and plays
562 a role in limiting oxidative stress in *Arabidopsis* spp. *Plant physiology* **169**(1): 549-559.
563 **Barberon M, Zelazny E, Robert S, Conejero G, Curie C, Friml J, Vert G. 2011.** Monoubiquitin-dependent
564 endocytosis of the iron-regulated transporter 1 (IRT1) transporter controls iron uptake in plants. *Proc*
565 *Natl Acad Sci USA* **108**(32): E450-458.
566 **Becher M, Talke IN, Krall L, Krämer U. 2004.** Cross-species microarray transcript profiling reveals high
567 constitutive expression of metal homeostasis genes in shoots of the zinc hyperaccumulator
568 *Arabidopsis halleri*. *The Plant journal : for cell and molecular biology* **37**(2): 251-268.
569 **Bert V, MacNair MR, De Laguérie P, Saumitou-Laprade P, Petit D. 2000.** Zinc tolerance and accumulation in
570 metallicolous and non metallicolous populations of *Arabidopsis halleri* (Brassicaceae). *The New*
571 *phytologist* **146**: 225-233.
572 **Bomblies K, Higgins JD, Yant L. 2015.** Meiosis evolves: adaptation to external and internal environments.
573 *The New phytologist* **208**(2): 306-323.
574 **Bouyer D, Heese M, Chen P, Harashima H, Roudier F, Gruttner C, Schnittger A. 2018.** Genome-wide
575 identification of RETINOBLASTOMA RELATED 1 binding sites in Arabidopsis reveals novel DNA
576 damage regulators. *PLoS genetics* **14**(11): e1007797.
577 **Briskine RV, Paape T, Shimizu-Inatsugi R, Nishiyama T, Akama S, Sese J, Shimizu KK. 2017.** Genome
578 assembly and annotation of *Arabidopsis halleri*, a model for heavy metal hyperaccumulation and
579 evolutionary ecology. *Molecular ecology resources* **17**(5): 1025-1036.
580 **Cailliatte R, Schikora A, Briat JF, Mari S, Curie C. 2010.** High-affinity manganese uptake by the metal
581 transporter NRAMP1 is essential for Arabidopsis growth in low manganese conditions. *Plant Cell*
582 **22**(3): 904-917.
583 **Callis J. 2014.** The ubiquitination machinery of the ubiquitin system. *The Arabidopsis book / American Society*
584 *of Plant Biologists* **12**: e0174.
585 **Corso M, Schvartzman MS, Guzzo F, Souard F, Malkowski E, Hanikenne M, Verbruggen N. 2018.** Contrasting
586 cadmium resistance strategies in two metallicolous populations of *Arabidopsis halleri*. *The New*
587 *phytologist* **218**(1): 283-297.
588 **Deinlein U, Weber M, Schmidt H, Rensch S, Trampczynska A, Hansen TH, Husted S, Schjoerring JK, Talke**
589 **IN, Krämer U, et al. 2012.** Elevated nicotianamine levels in *Arabidopsis halleri* roots play a key role
590 in zinc hyperaccumulation. *Plant Cell* **24**(2): 708-723.
591 **Dräger DB, Desbrosses-Fonrouge AG, Krach C, Chardonnens AN, Meyer RC, Saumitou-Laprade P, Krämer**
592 **U. 2004.** Two genes encoding *Arabidopsis halleri* MTP1 metal transport proteins co-segregate with
593 zinc tolerance and account for high *MTP1* transcript levels. *The Plant journal : for cell and molecular*
594 *biology* **39**(3): 425-439.
595 **Dubest S, Gallego ME, White CI. 2004.** Roles of the AtERCC1 protein in recombination. *The Plant journal :*
596 *for cell and molecular biology* **39**(3): 334-342.
597 **Duran-Figueroa N, Vielle-Calzada JP. 2010.** ARGONAUTE9-dependent silencing of transposable elements in
598 pericentromeric regions of Arabidopsis. *Plant signaling & behavior* **5**(11): 1476-1479.
599 **Ernst WHO. 1974.** *Schwermetallvegetationen der Erde*. Stuttgart, Germany: Gustav Fischer Verlag.
600 **Fernandes JB, Duhamel M, Seguela-Arnaud M, Froger N, Girard C, Choinard S, Solier V, De Winne N, De**
601 **Jaeger G, Gevaert K, et al. 2018.** FIGL1 and its novel partner FLIP form a conserved complex that
602 regulates homologous recombination. *PLoS genetics* **14**(4): e1007317.
603 **Geuting V, Kobbe D, Hartung F, Durr J, Focke M, Puchta H. 2009.** Two distinct MUS81-EME1 complexes from
604 Arabidopsis process Holliday junctions. *Plant physiology* **150**(2): 1062-1071.
605 **Grandbastien MA. 2015.** LTR retrotransposons, handy hitchhikers of plant regulation and stress response.
606 *Biochimica et biophysica acta* **1849**(4): 403-416.
607 **Halimaa P, Blande D, Baltzi E, Aarts MGM, Granlund L, Keinanen M, Karenlampi SO, Kozhevnikova AD,**
608 **Peraniemi S, Schat H, et al. 2019.** Transcriptional effects of cadmium on iron homeostasis differ in

609 calamine accessions of *Noccaea caerulescens*. *The Plant journal : for cell and molecular biology* **97**(2):
610 306-320.
611 **Hanikenne M, Talke IN, Haydon MJ, Lanz C, Nolte A, Motte P, Kroymann J, Weigel D, Krämer U. 2008.**
612 Evolution of metal hyperaccumulation required *cis*-regulatory changes and triplication of *HMA4*.
613 *Nature* **453**: 391-395.
614 **Hefner E, Preuss SB, Britt AB. 2003.** Arabidopsis mutants sensitive to gamma radiation include the
615 homologue of the human repair gene ERCC1. *Journal of experimental botany* **54**(383): 669-680.
616 **Honjo MN, Kudoh H. 2019.** *Arabidopsis halleri*: a perennial model system for studying population
617 differentiation and local adaptation. *AoB Plants* **11**(6).
618 **Horvath V, Merenciano M, Gonzalez J. 2017.** Revisiting the relationship between transposable elements and
619 the eukaryotic stress response. *Trends in genetics : TIG* **33**(11): 832-841.
620 **Hussain D, Haydon MJ, Wang Y, Wong E, Sherson SM, Young J, Camakaris J, Harper JF, Cobbett CS. 2004.**
621 P-type ATPase heavy metal transporters with roles in essential zinc homeostasis in Arabidopsis. *Plant*
622 *Cell* **16**(5): 1327-1339.
623 **Kazemi-Dinan A, Thomaschky S, Stein RJ, Krämer U, Müller C. 2014.** Zinc and cadmium hyperaccumulation
624 act as deterrents towards specialist herbivores and impede the performance of a generalist
625 herbivore. *The New phytologist* **202**(2): 628-639.
626 **Kerkeb L, Mukherjee I, Chatterjee I, Lahner B, Salt DE, Connolly EL. 2008.** Iron-induced turnover of the
627 Arabidopsis IRON-REGULATED TRANSPORTER1 metal transporter requires lysine residues. *Plant*
628 *physiology* **146**(4): 1964-1973.
629 **Kim D, Langmead B, Salzberg SL. 2015.** HISAT: a fast spliced aligner with low memory requirements. *Nature*
630 *methods* **12**(4): 357-360.
631 **Kovalchuk O, Titov V, Hohn B, Kovalchuk I. 2001.** A sensitive transgenic plant system to detect toxic
632 inorganic compounds in the environment. *Nature biotechnology* **19**(6): 568-572.
633 **Krämer U. 2015.** Planting molecular functions in an ecological context with *Arabidopsis thaliana*. *eLife* **4**.
634 **Krämer U. 2018.** Conceptualizing plant systems evolution. *Current opinion in plant biology* **42**: 66-75.
635 **Lamas GA, Navas-Acien A, Mark DB, Lee KL. 2016.** Heavy Metals, Cardiovascular Disease, and the
636 Unexpected Benefits of Chelation Therapy. *J Am Coll Cardiol* **67**(20): 2411-2418.
637 **Lämmli UK. 1970.** Cleavage of structural proteins during the assembly of the head of bacteriophage T4.
638 *Nature* **227**(5259): 680-685.
639 **Leskova A, Giehl RFH, Hartmann A, Fargasova A, von Wiren N. 2017.** Heavy Metals Induce Iron Deficiency
640 Responses at Different Hierarchic and Regulatory Levels. *Plant physiology* **174**(3): 1648-1668.
641 **Liu M, Ba Z, Costa-Nunes P, Wei W, Li L, Kong F, Li Y, Chai J, Pontes O, Qi Y. 2017.** IDN2 Interacts with RPA
642 and Facilitates DNA Double-Strand Break Repair by Homologous Recombination in Arabidopsis. *Plant*
643 *Cell* **29**(3): 589-599.
644 **Love MI, Huber W, Anders S. 2014.** Moderated estimation of fold change and dispersion for RNA-seq data
645 with DESeq2. *Genome biology* **15**(12): 550.
646 **Mercier R, Mezard C, Jenczewski E, Macaisne N, Grelon M. 2015.** The molecular biology of meiosis in plants.
647 *Annual review of plant biology* **66**: 297-327.
648 **Meyer CL, Juraniec M, Huguet S, Chaves-Rodriguez E, Salis P, Isaure MP, Goormaghtigh E, Verbruggen N.**
649 **2015.** Intraspecific variability of cadmium tolerance and accumulation, and cadmium-induced cell
650 wall modifications in the metal hyperaccumulator *Arabidopsis halleri*. *Journal of experimental*
651 *botany* **66**(11): 3215-3227.
652 **Meyer CL, Kostecka AA, Saumitou-Laprade P, Creach A, Castric V, Pauwels M, Frerot H. 2010.** Variability of
653 zinc tolerance among and within populations of the pseudometallophyte species *Arabidopsis halleri*
654 and possible role of directional selection. *The New phytologist* **185**(1): 130-142.
655 **Morales ME, Derbes RS, Ade CM, Ortego JC, Stark J, Deininger PL, Roy-Engel AM. 2016.** Heavy metal
656 exposure influences double strand break DNA repair outcomes. *PloS one* **11**(3): e0151367.
657 **Mortazavi A, Williams BA, McCue K, Schaeffer L, Wold B. 2008.** Mapping and quantifying mammalian
658 transcriptomes by RNA-Seq. *Nature methods* **5**(7): 621-628.
659 **Nagano AJ, Kawagoe T, Sugisaka J, Honjo MN, Iwayama K, Kudoh H. 2019.** Annual transcriptome dynamics
660 in natural environments reveals plant seasonal adaptation. *Nat Plants* **5**(1): 74-83.

661 **Nriagu JO, Pacyna JM. 1988.** Quantitative assessment of worldwide contamination of air, water and soils by
662 trace metals. *Nature* **333**(6169): 134-139.
663 **Okonechnikov K, Conesa A, Garcia-Alcalde F. 2016.** Qualimap 2: advanced multi-sample quality control for
664 high-throughput sequencing data. *Bioinformatics* **32**(2): 292-294.
665 **Oliver C, Santos JL, Pradillo M. 2014.** On the role of some ARGONAUTE proteins in meiosis and DNA repair
666 in *Arabidopsis thaliana*. *Frontiers in plant science* **5**: 177.
667 **Olmedo-Monfil V, Duran-Figueroa N, Arteaga-Vazquez M, Demesa-Arevalo E, Autran D, Grimanelli D,**
668 **Slotkin RK, Martienssen RA, Vielle-Calzada JP. 2010.** Control of female gamete formation by a small
669 RNA pathway in Arabidopsis. *Nature* **464**(7288): 628-632.
670 **Pauwels M, Saumitou-Laprade P, Holl AC, Petit D, Bonnin I. 2005.** Multiple origin of metallicolous
671 populations of the pseudometallophyte *Arabidopsis halleri* (Brassicaceae) in central Europe: the
672 cpDNA testimony. *Molecular ecology* **14**(14): 4403-4414.
673 **Pietzenuk B, Markus C, Gaubert H, Bagwan N, Merotto A, Bucher E, Pecinka A. 2016.** Recurrent evolution
674 of heat-responsiveness in Brassicaceae COPIA elements. *Genome biology* **17**(1): 209.
675 **R Core Team 2013**. R: A language and environment for statistical computing. Vienna, Austria: Foundation for
676 Statistical Computing.
677 **Reeves RD, Baker AJM, Jaffre T, Erskine PD, Echevarria G, van der Ent A. 2018.** A global database for plants
678 that hyperaccumulate metal and metalloid trace elements. *The New phytologist* **218**(2): 407-411.
679 **Reimand J, Arak T, Adler P, Kolberg L, Reisberg S, Peterson H, Vilo J. 2016.** g:Profiler-a web server for
680 functional interpretation of gene lists (2016 update). *Nucleic acids research* **44**(W1): W83-89.
681 **Robinson JT, Thorvaldsdottir H, Wenger AM, Zehir A, Mesirov JP. 2017.** Variant Review with the Integrative
682 Genomics Viewer. *Cancer Res* **77**(21): e31-e34.
683 **Rounds MA, Larsen PB. 2008.** Aluminum-dependent root-growth inhibition in Arabidopsis results from
684 AtATR-regulated cell-cycle arrest. *Current biology : CB* **18**(19): 1495-1500.
685 **Sakamoto T, Inui YT, Uraguchi S, Yoshizumi T, Matsunaga S, Mastui M, Umeda M, Fukui K, Fujiwara T. 2011.**
686 Condensin II alleviates DNA damage and is essential for tolerance of boron overload stress in
687 Arabidopsis. *Plant Cell* **23**(9): 3533-3546.
688 **Schat H, Ten Bookum WM. 1992.** Genetic control of copper tolerance in *Silene vulgaris*. *Heredity* **68**(3): 219-
689 229.
690 **Schuermann D, Molinier J, Fritsch O, Hohn B. 2005.** The dual nature of homologous recombination in plants.
691 *Trends in genetics : TIG* **21**(3): 172-181.
692 **Schvartzman MS, Corso M, Fataftah N, Scheepers M, Nouet C, Bosman B, Carnol M, Motte P, Verbruggen**
693 **N, Hanikenne M. 2018.** Adaptation to high zinc depends on distinct mechanisms in metallicolous
694 populations of *Arabidopsis halleri*. *The New phytologist* **218**(1): 269-282.
695 **Seeliger K, Dukowic-Schulze S, Wurz-Wildersinn R, Pacher M, Puchta H. 2012.** BRCA2 is a mediator of
696 RAD51- and DMC1-facilitated homologous recombination in *Arabidopsis thaliana*. *The New*
697 *phytologist* **193**(2): 364-375.
698 **Sinclair SA, Senger T, Talke IN, Cobbett CS, Haydon MJ, Kramer U. 2018.** Systemic upregulation of MTP2-
699 and HMA2-mediated Zn partitioning to the shoot supplements local Zn deficiency responses. *Plant*
700 *Cell* **30**(10): 2463-2479.
701 **Stein RJ, Höreth S, de Melo JR, Syllwasschy L, Lee G, Garbin ML, Clemens S, Krämer U. 2017.** Relationships
702 between soil and leaf mineral composition are element-specific, environment-dependent and
703 geographically structured in the emerging model *Arabidopsis halleri*. *The New phytologist* **213**(3):
704 1274-1286.
705 **Talke IN, Hanikenne M, Krämer U. 2006.** Zinc-dependent global transcriptional control, transcriptional
706 deregulation, and higher gene copy number for genes in metal homeostasis of the hyperaccumulator
707 *Arabidopsis halleri*. *Plant physiology* **142**(1): 148-167.
708 **Vaucheret H. 2008.** Plant ARGONAUTES. *Trends in plant science* **13**(7): 350-358.
709 **Vert G, Grotz N, Dedaldechamp F, Gaymard F, Guerinot ML, Briat JF, Curie C. 2002.** IRT1, an Arabidopsis
710 transporter essential for iron uptake from the soil and for plant growth. *Plant Cell* **14**(6): 1223-1233.
711 **Weber M, Harada E, Vess C, Roepenack-Lahaye EV, Clemens S. 2004.** Comparative microarray analysis of
712 *Arabidopsis thaliana* and *Arabidopsis halleri* roots identifies nicotianamine synthase, a ZIP

713 transporter and other genes as potential metal hyperaccumulation factors. *The Plant journal : for*
714 *cell and molecular biology* **37**: 269-281.
715 **Weber M, Trampczynska A, Clemens S. 2006.** Comparative transcriptome analysis of toxic metal responses
716 in *Arabidopsis thaliana* and the Cd(2+)-hypertolerant facultative metallophyte *Arabidopsis halleri*.
717 *Plant Cell Environ* **29**(5): 950-963.
718 **Yant L, Hollister JD, Wright KM, Arnold BJ, Higgins JD, Franklin FC, Bomblies K. 2013.** Meiotic adaptation to
719 genome duplication in *Arabidopsis arenosa*. *Current Biology* **23**(21): 2151-2156.

720

721

722 **Table 1.** List of genes in overrepresented meiosis- and homologous recombination-related GOs (see Fig. 3a, b).

						log_2FC[b]	
Name	**Description**	**AGI**	**Aha Id.**	**GO**[a]	**Somatic DNA repair in *A. thaliana***	**Max**	**Min**
AGO9	Argonaute 9	AT5G21150	g12002	Meiosis	Oliver *et al*., 2014	6.57 ***	3.88 ***
ZYP1a	Zipper-like 1a	AT1G22260	g13785	Meiosis/HR	n.i.[c]	4.84 ***	1.55 **
ZYP1b	Zipper-like 1b	AT1G22275	g13782	Meiosis/HR	n.i.	3.73 ***	2.44 ***
EMB2656	Embryo defective 2656	AT5G37630	g20599	HR	n.i.	3.31 ***	1.01 ***
SMC2	Structural maintenance of chromosomes 2	AT3G47460	g12815	Meiosis	n.i.	1.98 ***	1.12 *
SWI1	SWITCH1	AT5G51330	g08416	Meiosis	n.i.	1.89 **	1.08 *
ERCC1	DNA excision repair protein ERCC-1	AT3G05210	g06284	Meiosis	Dubest *et al*., 2004	1.63 ***	0.56 *
MSH5	MUTS-homologue 5	AT3G20475	g11121	Meiosis/HR	n.i.	1.60 ***	1.04 **
PRD3	Putative recombination initiation defects 3	AT1G01690	g01742	Meiosis	n.i.	1.60 ***	1.05 *
EME1A	Essential meiotic endonuclease 1A	AT2G21800	g23988	Meiosis	Geuting *et al*., 2009	1.59 ***	0.72 *
BRCA2B	Breast cancer susceptibility 2 homolog B	AT5G01630	g27928	Meiosis/HR	Kumar *et al*., 2019; Seeliger *et al*., 2012	1.54 ***	-0.91 ***
NA	WEB family protein	AT3G02930	g31838	Meiosis/HR	n.i.	1.47 ***	0.55 ***
NA	Eisosome protein	AT1G04030	g02033	Meiosis	n.i.	1.39 ***	0.80 **
RPA2B	Replication protein A, subunit RPA32	AT3G02920	g02469	Meiosis/HR	Liu *et al*., 2017	1.37 ***	0.98 ***
MHF2	MPH1-associated histone-fold protein 2	AT1G78790	g01439	Meiosis	n.i.	1.32 ***	0.58 *
CAP-D3	Condensin-2 complex subunit D3	AT4G15890	g20215	Meiosis/HR	n.i.	1.26 *	0.94 *
MCM8	Minichromosome maintenance 8	AT3G09660	g06091	Meiosis	n.i.	1.21 **	0.82 *
ATK1	*Arabidopsis thaliana* knotted-like 1	AT4G21270	g29731	Meiosis/HR	n.i.	1.15 ***	0.70 **
SMC3	Structural maintenance of chromosome 3	AT5G48600	g15955	Meiosis	n.i.	1.13 ***	0.46 *
FLIP	Fidgetin-like-1 interacting protein	AT1G04650	g02098	Meiosis	Fernandes *et al*., 2018; Bouyer et al., 2018	1.06 **	0.93 *
HEB2	Hypersensitive to excess boron 2	AT3G16730	g06531	HR	Sakamoto *et al*., 2011	0.88 ***	0.40 *
ESP	Extra spindle poles	AT4G22970	g14375	Meiosis	n.i.	0.82 **	0.42 *
EME1B	Essential meiotic endonuclease 1B	AT2G22140	g28064	Meiosis	Geuting *et al*., 2009	0.70 ***	0.35 **

723 [a]Meiosis, meiotic cell cycle or meiosis I cell cycle process; HR, homologous recombination (reciprocal meiotic recombination).
724 [b]Maximum and minimum of Log_2(fold change Noss *vs*. any population from an NM site) across all tissues and conditions (adjusted *P*-value < 0.001, ***; < 0.01, **; <
725 0.05, *). [c]Not identified.
726

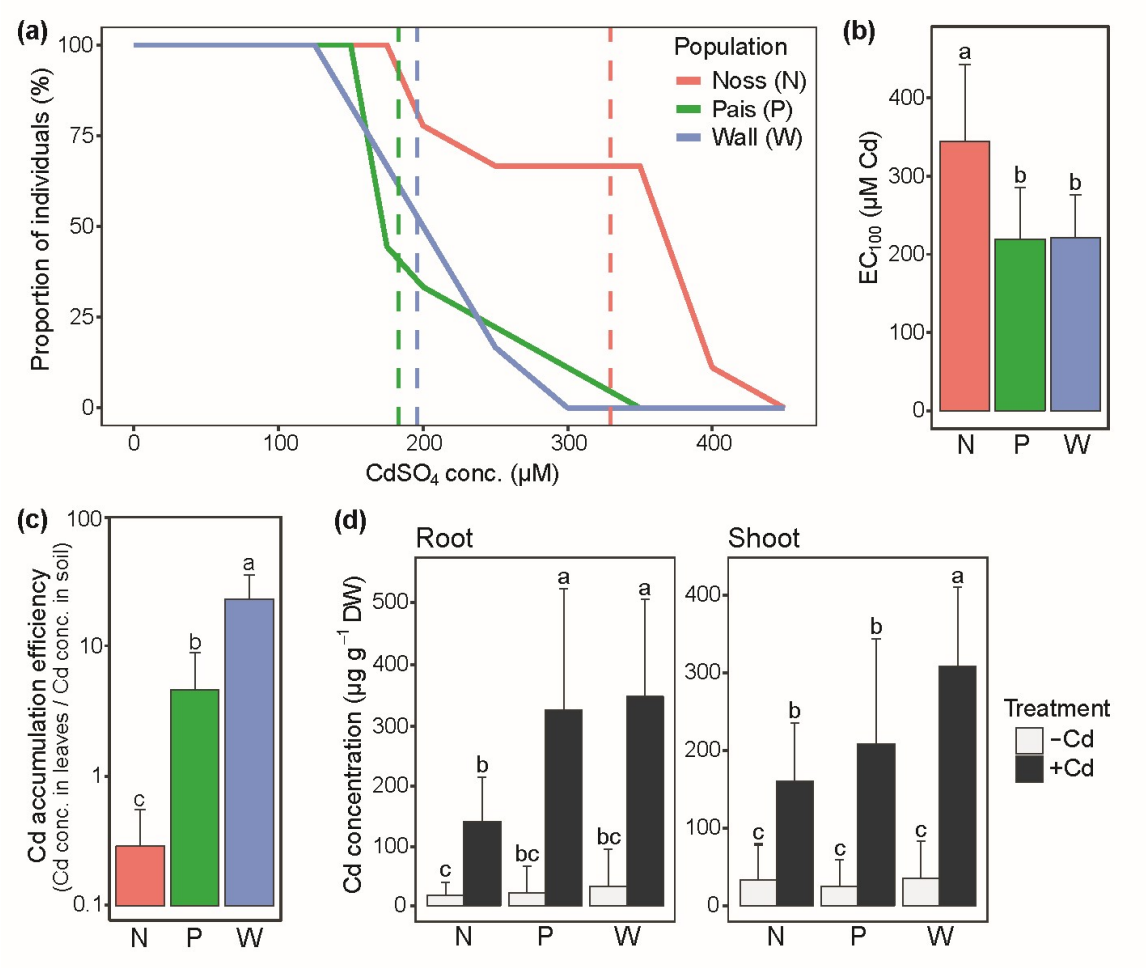

Figure 1. Cadmium tolerance and accumulation in three populations of *A. halleri*. (a) Proportion of individuals maintaining root growth (elongation) as a function of Cd concentration. Dashed vertical lines indicate ED_{50}, the effective dose required to reach a proportion of 50% according to a dose-response model (see Table S2, Figure S1). (b) Cd tolerance index. Bars represent mean ± SD of EC_{100} (effective Cd concentration causing 100% root growth inhibition) in a given plant individual (Schat and Ten Bookum, 1992). Plants were sequentially exposed to stepwise increasing concentrations of $CdSO_4$ in hydroponic culture every week (n = 6 to 9 per population, with one to three vegetative clones of each three to six genotypes per population; (a, b)). (c) Cd accumulation efficiency at the site of origin calculated from published field survey data (bars represent means ± SD of n = 11 to 12 individuals in the field; units employed, µg Cd g^{-1} dry biomass in leaves, µg total Cd g^{-1} dry mass in soil; data from Stein et al. 2017). (d) Cd concentration in root and shoot tissues of hydroponically cultivated plants. Shown are mean ± SD (n = 12 to 20 clones per population comprising both genotypes, from all three replicate experiments; see Supplemental Table 1). Four-week-old vegetative clones were exposed to 0 (-Cd) and 2 µM $CdSO_4$ (+Cd) in hydroponic culture for 16 d alongside the plants cultivated for RNA-seq. Different characters denote statistically significant differences between means based on two-way ANOVA, followed by Tukey's HSD test (Log-transformed data were used in (c)) (P < 0.05; see Supplemental Table 3, for nested ANOVA of genotypes within a population (d)).

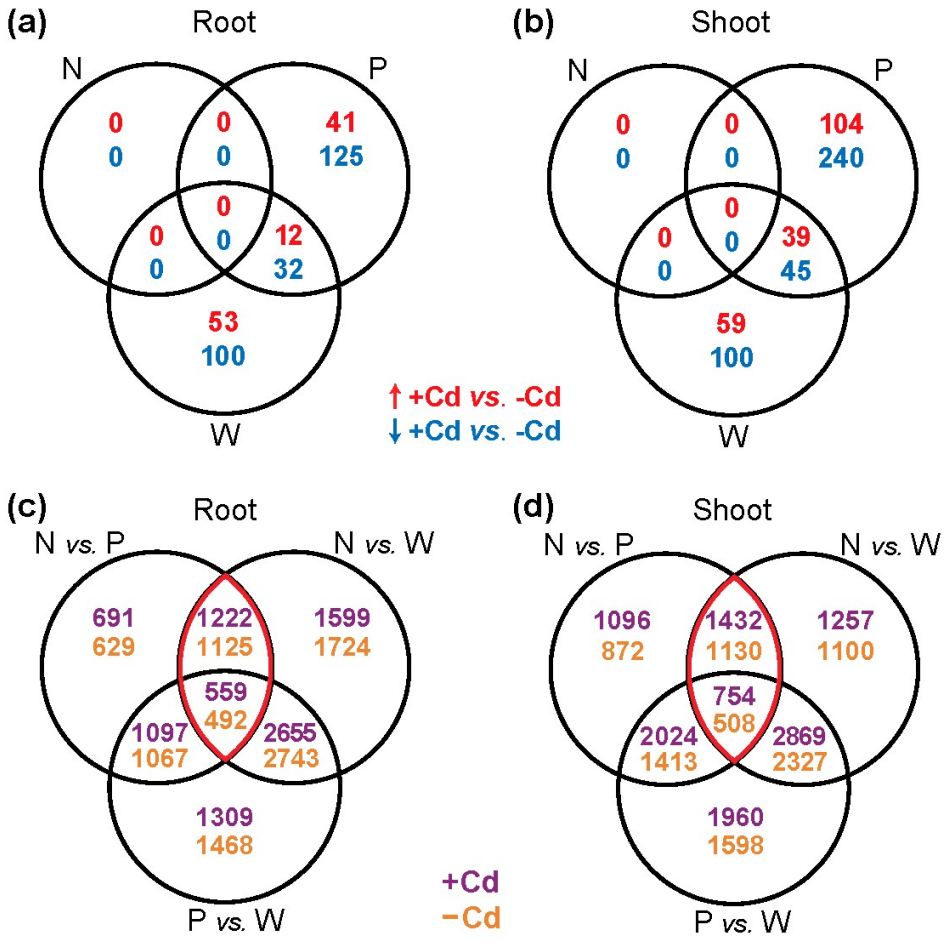

Figure 2. Between-population differences according to transcriptome sequencing. (a, b) Venn diagrams show the numbers of genes exhibiting differential transcript abundances under exposure to Cd (+Cd) compared to control conditions (-Cd) for the three populations Noss (N), Pais (P) and Wall (W) in root (a) and shoot (b) tissues. Upregulation (red): Log_2(fold change +Cd *vs.* –Cd) = $Log_2FC > 0.5$; downregulation (blue): $Log_2FC < -0.5$; all with adjusted *P*-value < 0.05. (c, d) Venn diagrams show the numbers of genes exhibiting differential transcript abundance between populations in root (c) and shoot (d) tissues of plants cultivated under Cd exposure (violet) or control conditions (orange) ($|Log_2FC| > 0.5$; adjusted *P*-value < 0.05). Red lines surround genes differentially expressed between Noss and both populations of NM soils (Pais and Wall). Four-week-old vegetative clones were exposed to 2 µM Cd or 0 µM Cd (controls) in hydroponic culture for 16 d before harvest. Data are from three independent experiments (repeats), with two genotypes per population and material pooled from six replicate vegetative clones (three hydroponic culture vessels) per genotype in each experiment.

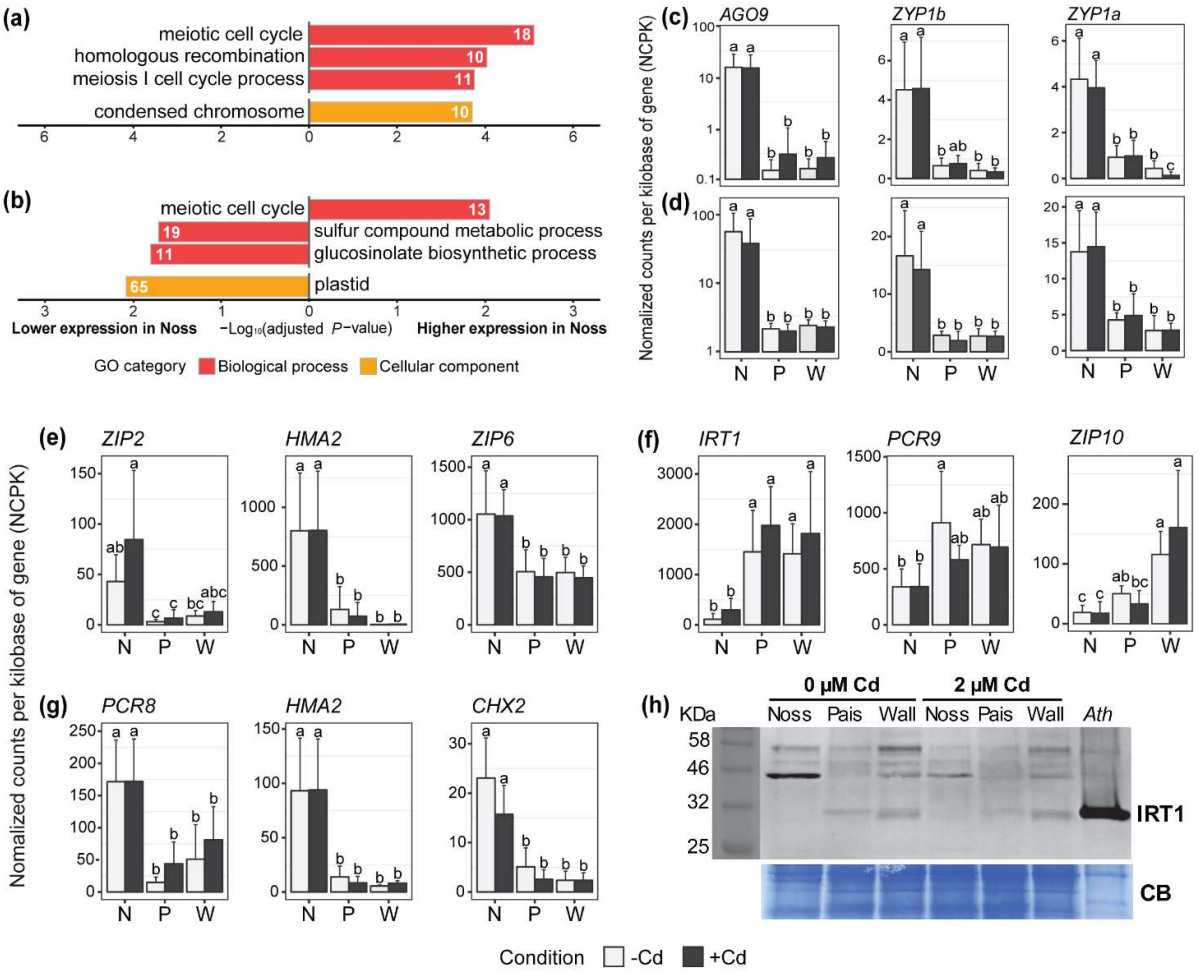

Figure 3. Candidate genes differentially expressed in Noss compared to both other populations Pais and Wall. (a, b) Significantly enriched gene ontology (GO) categories for roots (a) and shoots (b) of plants cultivated in 0 μM Cd (see Figure 2c and d, Dataset S3). Genes differentially expressed between Noss from M soil and both Pais and Wall from NM soils were subjected to a GO term enrichment analysis. The number of genes in each over-represented category is shown inside bars (see Dataset S4 for all genes). (c, d) Relative transcript levels of the top three genes (largest between-population differences) taken from (a) and (b) in the over-represented GO category meiotic cell cycle, for roots (c) and shoots (d). (e-g) Relative transcript levels of metal homeostasis genes of which transcript levels are high (e, g) and low (f) in Noss (N) compared to both Pais (P) and Wall (W), for roots (e, f) and shoots (g) (top three genes from Table S8). Bars show means ± SD (n = 6) of normalized counts, which were additionally normalized per kilobase of gene length (NCPK). Different characters represent statistically significant groups based on two-way ANOVA, followed by Tukey's HSD test ($P < 0.05$, see Table S6, for details). Data are from the same experiment as shown in Figure 2. (H) Immunoblot of IRT1. Total protein extracts (40 μg) from roots of Noss_05, Pais_09 and Wall_07 were separated on a denaturing polyacrylamide gel, blotted, and detection was carried out using an anti-IRT1 antibody. Total protein extract (10 μg) from roots of Fe- and Zn-deficient *A. thaliana* (*Ath*, right lane) served as a positive control, with IRT1 detected as a single band at *ca*. 31 kDa. In *A. halleri*, additional bands at *ca*. 44, 48 and 56 kDa are likely to constitute non-specific ross-reactions of the antibody. Coomassie Blue (CB) stained membrane is shown as a loading control.

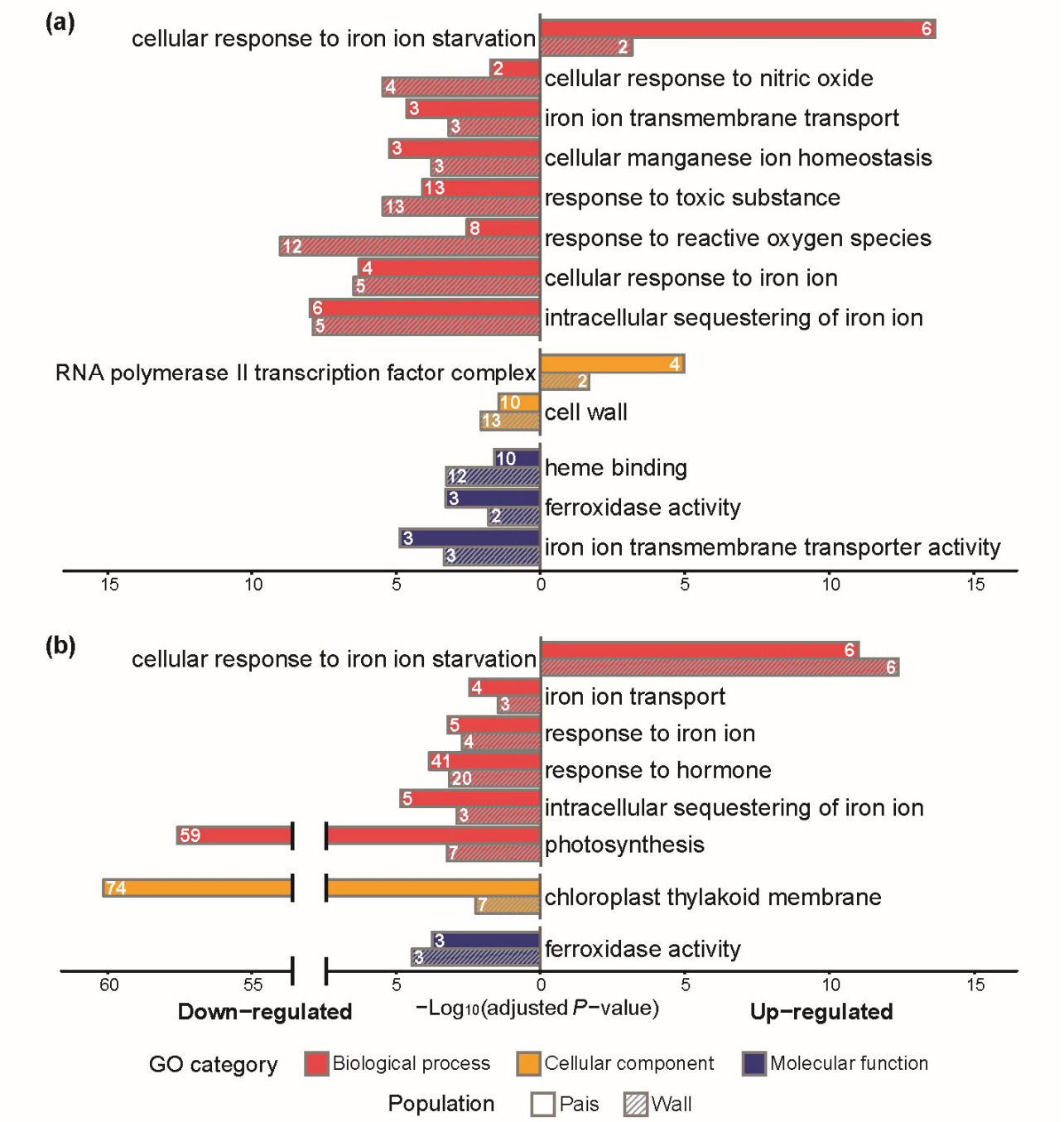

Figure 4. Functional classification of the transcriptional Cd responses in less metal-tolerant populations from NM sites. Significantly enriched GO categories among the transcriptional responses to Cd common in both the Pais and Wall populations for (a) roots and (b) shoots (see Figure 2a and b, Dataset S6). The numbers of genes in each over-represented category are shown inside bars. Data are from the same experiment as shown in Figure 2.

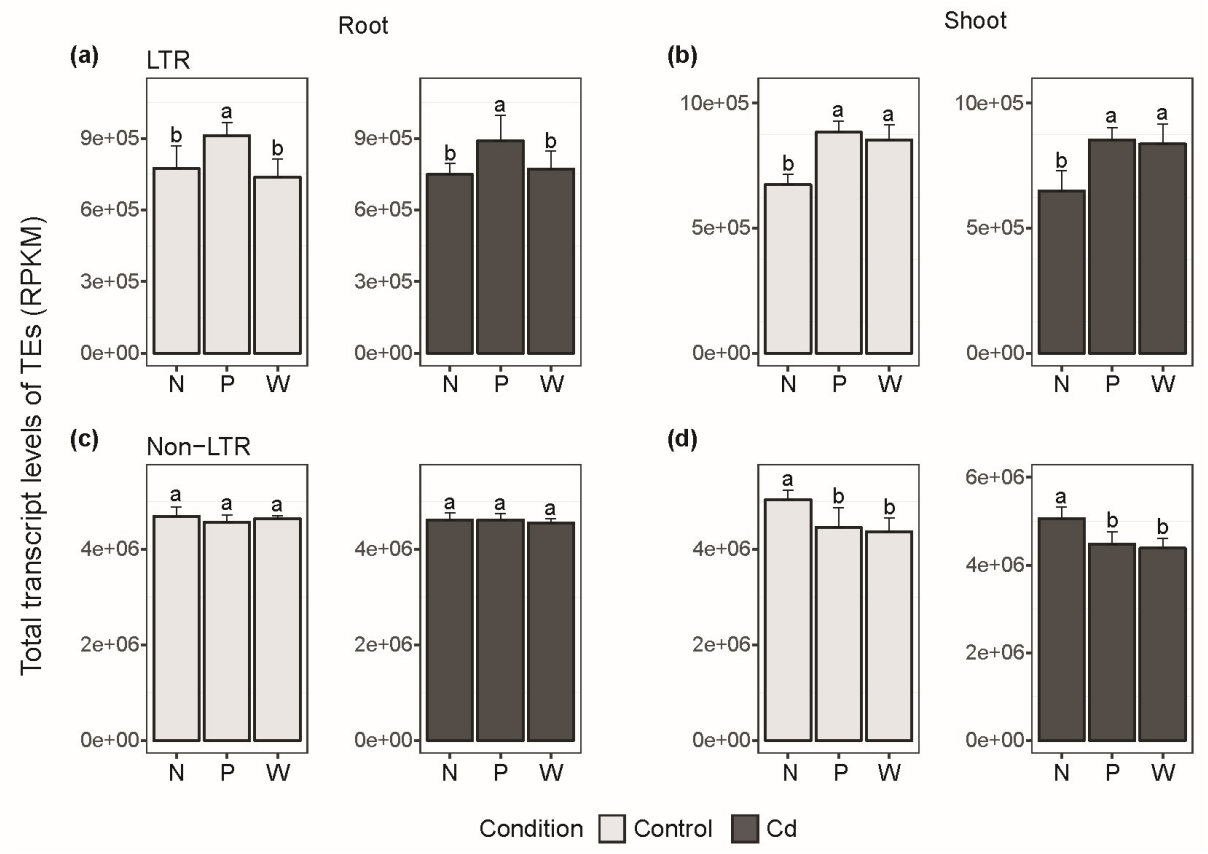

Figure 5. Genome-wide sum of transcript levels contributed by different types of transposable elements in Noss, Pais and Wall. (a-d) Bars show means ± SD (n = 6) of transcript levels of transposable elements (TEs), corresponding to the sum total of RPKM for LTR (Long terminal repeat) retrotransposons (a, b) and non-LTR TEs (c, d) in root (a, c) and shoot (b, d), with RPKM ≥ 7 per locus. Different characters represent statistically significant differences based on one-way ANOVA, followed by Tukey's HSD test (P < 0.05).

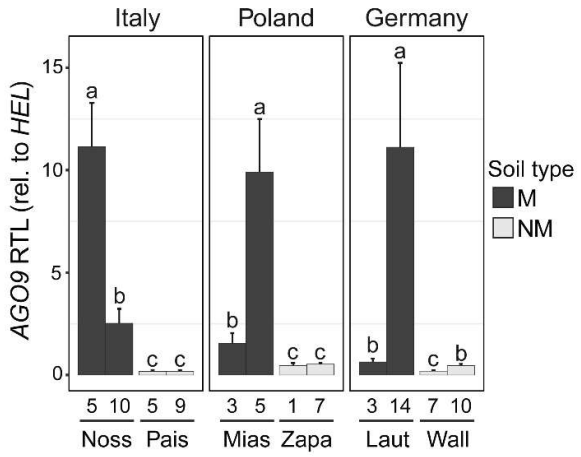

Figure 6. *ARGONAUTE 9* (*AGO9*) transcript levels in *A. halleri* individuals originating from metalliferous and non-metalliferous soils in Italy, Poland and Germany. Bargraph shows mean ± SD (n = 4) of relative *AGO9* transcript levels quantified by RT-qPCR in leaves of 5.5-week-old vegetative clones cultivated hydroponically (technical replicates, with two independent PCR runs on each of two independently synthesized cDNAs from a pool of six replicate clones). Data are shown relative to the constitutively expressed gene *Helicase* (*HEL*). Each PCR reaction was conducted in hexuplicate. Different characters represent statistically significant differences based on one-way ANOVA, followed by Tukey's HSD test ($P < 0.05$). For details on collection sites and individuals see Stein et al., 2017.